PERGAMON

International Journal of Heat and Mass Transfer 45 (2002) 4507–4514

International Journal of HEAT and MASS TRANSFER

www.elsevier.com/locate/ijhmt

# Mass transfer by free and forced convection from single spherical liquid drops

M. Adekojo Waheed [a,*], Martin Henschke [b], Andreas Pfennig [b]

[a] *Department of Mechanical Engineering, Ladoke Akintola University of Technology, P.M.B. 4000 Ogbomoso, Oyo State, Nigeria*
[b] *Lehrstuhl für Thermische Verfahrenstechnik, RWTH Aachen, Wüllnerstrasse 5, D-52056 Aachen, Germany*

Received 4 July 2001; received in revised form 27 March 2002

## Abstract

Numerical simulations of the mass-transfer of droplet in a continuous phase were done for a conjugate problem. The effect of free and combined convection on the mass transfer was investigated by solving the governing equations using the finite element method. The results show that the mass transfer depends very strongly on the flow conditions. The effect of free convection on mass transfer at high Reynolds number is small. The mass transfer by the combined free and forced convection for a rising drop was found to be smaller than that for a falling drop. The simulation was limited to $Re_c \leqslant 20$.

*Keywords:* Mass transfer; Mass-transfer coefficient; Liquid drop; Liquid–liquid extraction; Free convection; Force convection

## 1. Introduction

In this work, the effect of free convection on the unsteady-state mass transfer of liquid drop was investigated. Liquid drops occur in many engineering applications including the liquid–liquid extraction equipment where one of the liquid phases is dispersed in the form of liquid droplets into another phase. The two phases are in most cases immiscible or partially miscible with each other. This method of contact results in a large interfacial area per unit volume of mass transfer and thus enhances the separation process. The knowledge of the relevant fluid dynamics and of the mass transfer in a single drop is, however, the basis for the estimation of the mass transfer in a system with many liquid droplets and hence is of paramount importance for the design of an extraction equipment [1]. A vast number of work published over the years in this field of study reflects the importance of the area to many industrial separation processes. In the previous work, the effect of flow condition (i.e. forced convection) [2,3] and of the Marangoni convection (i.e. convection induced by mass transfer) [4,5] on the mass transfer was investigated. A thorough understanding of all these mechanisms is needed for the quantitative prediction of the mass transfer coefficient. But this still proves difficult till date. That explains the reason why many empirical and idealized theoretical equations for predicting the mass transfer coefficient for drops in the literature do not generally reliably predict values in close agreement with those found experimentally [1,6].

Extensive theoretical, numerical and experimental work has been carried out on the continuous phase mass transfer to and from a liquid drop. The basis of the theoretical and numerical work is the solution of the flow and the convection–diffusion equations. Due to the inherent difficulty in the analytical solution of the complete flow equations, the theoretical investigation of the mass transfer has been limited to the creeping [7–9] and to the potential flow [6,10,11]. Boundary layer theory has also been used to describe the effect of forced convection on the mass transfer [12,13]. Both the boundary layer and the potential flow models are valid for high Reynolds number flow.

The solution of the unsteady-state mass transfer problem between a dispersed and a continuous phase is determined by the ratio of the diffusion coefficient

---

[*] Corresponding author.

0017-9310/02/$ - see front matter © 2002 Elsevier Science Ltd. All rights reserved.
PII: S0017-9310(02)00124-2

**Nomenclature**

| | |
|---|---|
| $A$ | area of projection of a drop, m$^2$ |
| $\vec{B}$ | body force, N |
| $D$ | diffusion coefficient, m$^2$/s |
| $D^* = D_\mathrm{d}/D_\mathrm{c}$ | ratio of diffusion coefficient |
| $d_\mathrm{d}$ | diameter of the drop, m |
| $\boldsymbol{F}$ | matrix for the boundary conditions |
| $Fo$ | Fourier number |
| $g$ | acceleration due to gravity, m/s$^2$ |
| $K$ | equilibrium distribution coefficient |
| $L^\mathrm{T}$ | continuity matrix |
| $\boldsymbol{M}_p$ | pressure matrix |
| $\boldsymbol{N}(\vec{u})$ | matrix of the discretized convective term |
| $p$ | pressure, N/m$^2$ |
| $r$ | horizontal coordinate |
| $R$ | radius of the drop, m |
| $Re$ | Reynolds number |
| $\boldsymbol{S}$ | stress matrix |
| $Sh$ | Sherwood number |
| $t$ | time, s |
| $\vec{u}$ | vector of unknown velocities $u_r$ and $u_z$, m/s |
| $u_r$ | horizontal velocity, m/s |
| $u_z$ | vertical velocity, m/s |
| $u_\infty$ | velocity at infinitely far distance from drop, m/s |
| $w_\mathrm{A}$ | concentration of solute A |
| $\bar{w}_\mathrm{A}$ | average concentration of solute A |
| $\bar{w}^*$ | dimensionless concentration |
| $z$ | vertical coordinate |

*Greek symbols*

| | |
|---|---|
| $\beta$ | mass-transfer coefficient, m/s |
| $\beta_\mathrm{K}$ | mass expansion coefficient |
| $\tau = 1/\varepsilon$ | penalty parameter |
| $\eta$ | viscosity, kg/ms |
| $\rho$ | density, kg/m$^3$ |
| $\psi$ | stream function, m$^3$/s |

*Subscripts*

| | |
|---|---|
| c | continuous phase |
| d | dispersed phase |
| A | solute A |

$D^* = D_\mathrm{d}/D_\mathrm{c}$. Three cases are to be distinguished from one another. When the parameter $D^* \ll 1$, then the rate of mass transfer is controlled by the transfer resistance in the dispersed phase (i.e. the internal problem). For external problem, the transfer resistance is limited to the continuous phase (i.e. $D^* \gg 1$). The third case is a conjugate problem in which the mass-transfer resistance between the two phases are comparable, i.e. $D \sim 1$ [14,15]. The mass-transfer resistance both in the continuous and the dispersed phases for many system used in liquid–liquid extraction is mostly of the same order. A conjugate problem is consequently investigated in this work.

The analytical solution of the unsteady state convection–diffusion equation is only limited to stagnant drop and to high Reynolds number flow. Gröber [7] was the first to present an analytical model for the unsteady mass-transfer process of a conjugate problem for a stagnant drop. Newton [8] adapted this model for an internal problem. Kronig and Brink [10] presented a model for the unsteady state mass-transfer process for a liquid drop with internal circulation by using the velocity field separately derived by Hadamard [16] and Rybczynski [17]. The dispersed phase mass-transfer coefficient $\beta_\mathrm{d}$ of a liquid drop with internal circulation with mass-transfer resistance in the drop is given according to the model as:

$$\beta_\mathrm{d} = -\frac{d_\mathrm{d}}{6t} \ln \left[ \frac{3}{8} \sum_{n=1}^{\infty} B_n^2 \exp\left( -\frac{64\lambda_n D_\mathrm{d} t}{d_\mathrm{d}^2} \right) \right]. \tag{1}$$

In this equation, $d_\mathrm{d}$ denoted the drop diameter, $D_\mathrm{d}$ the diffusion coefficient for the dispersed phase and $t$ the time. $B_n$ and $\lambda_n$ represent the eigenvalues and coefficients for Eq. (1). The values of these parameters can be obtained from Kronig and Bring [10] and from Elzinga and Bachero [18]. The long time solution of Eq. (1) is given as:

$$\beta_\mathrm{d} = 17.7 \frac{D_\mathrm{d}}{d_\mathrm{d}}. \tag{2}$$

In the past, many researchers [19–22] have investigated the effect of free, and combined free and forced convection on the steady-state mass transfer of a liquid drop. Their results, though at variance with one another, show that free convection plays a significant role on the continuous phase mass transfer process. But due to the relatively small size of a liquid drop and its limited potential to store material, both the mass transfer by free and combined convection in the dispersed phase should be investigated in an unsteady-state transfer process.

The main objective of this work is thus to simulate the unsteady-state mass transfer of a liquid drop. Boussinesq-approximation is thereby used to account for the change in density due to concentration changes. Further investigation included the simulation of the combined free and forced convection for falling and rising drops. The effect of combined convection on mass transfer was clearly shown by comparing the mass transfer by combined convection with that by forced convection. The simulation is limited to $Re_\mathrm{c} \leqslant 20$ because the effect of free convection is significant only in this flow regime.

## 2. Model equations

### 2.1. The flow equations

For the purpose of the numerical simulation of the motion and the mass transfer to and from a liquid drop in a continuous phase, a suspended liquid drop situated in a flowing unbounded fluid is considered instead of a falling or rising droplet. The flow at far away distance to the drop is uniform and its velocity is $u_\infty$. The drop has a constant diameter $d_\mathrm{d}$, density $\rho_\mathrm{d}$ and viscosity $\eta_\mathrm{d}$. The continuous phase has different density $\rho_\mathrm{c}$ and viscosity $\eta_\mathrm{c}$. Mass transfer takes place between the dispersed and the continuous phases as a result of concentration difference between them. The diffusion coefficient in the dispersed and continuous phases are represented by $D_\mathrm{d}$ and $D_\mathrm{c}$ respectively. Fig. 1 depicts the drop with the transport properties and the coordinates system. The flow in and around the drop is assumed to be axisymmetric and is described by the full incompressible Navier–Stokes equations [23,24]:

$$\rho\left[\frac{\partial\vec{v}}{\partial t}+(\vec{v}\nabla)\vec{v}\right]=-\nabla p+\eta\Delta\vec{v}+\vec{B} \tag{3}$$

and the continuity equation

$$\frac{\partial\rho}{\partial t}+(\nabla\cdot\rho\vec{v})=0. \tag{4}$$

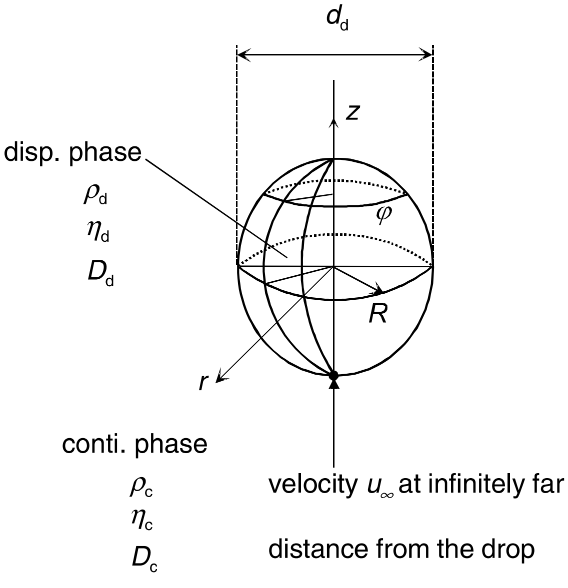

Fig. 1. Definition of control volume and the coordinates system.

$\vec{B}$, $p$ and $\vec{v}$ in the above equations respectively represent the body force, pressure and velocity vectors.

A slight change in density as a result of changes in concentration is allowed, so that free convection plays a significant role in the mass transfer process. The requirement for the occurrence of such flow is that the body force and the density gradient should not be parallel to each other. The change in density due to concentration changes is approximated using the Boussinesq-approximation [25,26] as

$$\rho=\rho_\infty-\rho_\infty\beta_\mathrm{K}(w-w_\infty). \tag{5}$$

In this equation, $\rho_\infty$ and $w_\infty$ represent the density and the concentration at reference state, $w$ denotes the concentration at a point and $\beta_\mathrm{K}$ the mass expansion coefficient. The body force is defined as the product of density $\rho$ and the acceleration due to gravity $g$:

$$\vec{B}=-\rho_\infty\vec{g}[1-\beta_\mathrm{K}(w-w_\infty)]=-\rho_\infty\vec{g}[1-\beta_\mathrm{K}\Delta w]. \tag{6}$$

The unsteady flow inside and outside a liquid drop is described by the Navier–Stokes equations in the cylindrical coordinates system modified for natural convection as follows

$$\rho\left(\frac{\partial u_r}{\partial t}+u_r\frac{\partial u_r}{\partial r}+u_z\frac{\partial u_r}{\partial z}\right)=-\frac{\partial p}{\partial r}+\eta\left(\frac{\partial^2 u_r}{\partial r^2}+\frac{1}{r}\frac{\partial u_r}{\partial r}+\frac{\partial^2 u_r}{\partial z^2}-\frac{u_r}{r^2}\right) \tag{7}$$

and

$$\rho\left(\frac{\partial u_z}{\partial t}+u_r\frac{\partial u_z}{\partial r}+u_z\frac{\partial u_z}{\partial z}\right)=-\frac{\partial p}{\partial z}+\eta\left(\frac{\partial^2 u_z}{\partial r^2}+\frac{1}{r}\frac{\partial u_z}{\partial r}+\frac{\partial^2 u_z}{\partial z^2}\right)-\rho_\infty g\beta_\mathrm{K}\Delta w \tag{8}$$

and the continuity equation in the same coordinates is

$$\frac{\partial\rho}{\partial t}+\frac{1}{r}\frac{\partial}{\partial r}(ru_r)+\frac{\partial u_z}{\partial z}=0. \tag{9}$$

The study of the unsteady laminar flow of an incompressible Newtonian fluid past a liquid drop requires the solution of the above stated equations subject to the prevailing boundary conditions. These conditions are: (i) The flow is assumed to be symmetric with respect to the $z$-axis. (ii) The interface between the drop and the surrounding fluid is assumed smooth. The size of the drop is constant and its shape is spherical. That means that the normal velocities of both fluids at the interface must be zero and that the tangential velocities are equal. (iii) The velocity of fluid inside the drop at $r=0$ must remain finite, $u_r=0$, $u_z\neq 0$. (iv) The tangential stresses at the interface between the two fluids must be equal. (v) The inflow velocity at sufficiently far distance from the drop is given as $u_\infty$.

The field of a flowing fluid is normally presented in a graphical form through the use of streamline, line of constant value of stream function $\psi$. Between two streamlines flows a stream of constant volume flow rate. For cylindrical coordinates system, the velocity components are defined as the partial differentials of the stream function as follows [27]:

$$u_r = \frac{\partial \psi}{2\pi r \partial z} \tag{10}$$

and

$$u_z = -\frac{\partial \psi}{2\pi r \partial r}. \tag{11}$$

By integrating Eqs. (10) and (11) the stream function at a point is obtained as:

$$\psi = \int_0^z 2\pi r u_r \, \mathrm{d}z \tag{12}$$

or

$$\psi = -\int_0^r 2\pi r u_z \, \mathrm{d}r. \tag{13}$$

### 2.2. Convection–diffusion equation

In this work, a dispersed and a continuous phase is considered to be a binary system consisting of a solvent and a solute. The initial concentration of the diffusing solute A in the drop is uniform and is equal to $w_{\mathrm{Ad0}}$, and the initial concentration in the continuous phase is given as $w_{\mathrm{Ac}\infty}$. Mass transfer thus occurs between the two phases as a result of concentration gradient. This process is governed by the convection–diffusion equation. The equation in cylindrical coordinates for a system without chemical reaction is stated below:

$$\frac{\partial w_{\mathrm{A}}}{\partial t} + u_r \frac{\partial w_{\mathrm{A}}}{\partial r} + u_z \frac{\partial w_{\mathrm{A}}}{\partial z} = D\left\{ \frac{1}{r}\frac{\partial}{\partial r}\left( r \frac{\partial w_{\mathrm{A}}}{\partial r} \right) + \frac{\partial^2 w_{\mathrm{A}}}{\partial z^2} \right\}. \tag{14}$$

The velocity components $u_r$ and $u_z$ are obtained from the solution of the continuity and the Navier–Stokes equations. Eq. (14) is valid for the description of the mass-transfer processes both in the dispersed and the continuous phases. This equation is subject to the initial and boundary conditions based on the assumptions of equilibrium at the droplet interface:

$$K\rho_{\mathrm{d}} D_{\mathrm{d}} \left.\frac{\partial w_{\mathrm{Ad}}}{\partial n}\right|_i = \rho_{\mathrm{c}} D_{\mathrm{c}} \left.\frac{\partial w_{\mathrm{Ac}}}{\partial n}\right|_i, \tag{15}$$

$$w_{\mathrm{Adp}} = K w_{\mathrm{Acp}}. \tag{16}$$

The parameter $K$ represents the equilibrium distribution coefficient. Its value depends on the type of problem. For an internal problem, $K < 1$ and for external problem $K > 1$. For a conjugate problem, $K$ is of order of unity. Since this work is concerned with a conjugate problem, $K$ in Eq. (16) is thus set equal to unity for all computations.

The following conditions are valid at the symmetry line:

$$\left.\frac{\partial w_{\mathrm{Ac}}}{\partial r}\right|_{r=0} = 0; \qquad \left.\frac{\partial w_{\mathrm{Ac}}}{\partial z}\right|_{r=0} \neq 0. \tag{17}$$

### 2.3. Mass-transfer coefficient and Sherwood number

The potential for mass transfer between two phases can be obtained quantitatively through the mean concentration $\bar{w}_{\mathrm{A}}$. But the actual transfer rate can be computed from the material balance at the interface. Mass transfer is normally quantified in practice in dimensionless form as Sherwood number, here defined for the dispersed phase $Sh_{\mathrm{d}}$:

$$Sh_{\mathrm{d}} = \frac{\beta_{\mathrm{d}} d_{\mathrm{d}}}{D_{\mathrm{d}}}. \tag{18}$$

The dimensionless mean concentration $\bar{w}^*_{\mathrm{d}}$, the average Sherwood number and the dimensionless time, the Fourier number $Fo_{\mathrm{d}}$ for the dispersed phase, are related through the following expression [14,28,29]:

$$\bar{w}^*_{\mathrm{d}} = 1 - \tfrac{3}{2} Sh_{\mathrm{d}} Fo_{\mathrm{d}}. \tag{19}$$

$\bar{w}^*_{\mathrm{d}}$ is defined as:

$$\bar{w}^*_{\mathrm{d}} = \frac{\bar{w}_{\mathrm{Ad}} - K w_{\mathrm{Ac}\infty}}{w_{\mathrm{Ad0}} - K w_{\mathrm{Ac}\infty}} \tag{20}$$

and the Fourier number for the dispersed phase is defined as:

$$Fo_{\mathrm{d}} = \frac{4 D_{\mathrm{d}} t}{d_{\mathrm{d}}^2}. \tag{21}$$

## 3. Solution method

The flow Eqs. (7)–(9) and the convection–diffusion equation (14) were solved numerically together with the prescribed initial and boundary conditions by the finite-element method. A CFD-Code SEPRAN [30] was used. This programme makes use of the penalty method [30,31]. The main advantages of this method over the integrated method are that the system of equations to be solved is appreciably reduced and that the problem with zero pivots is avoided. Consequently, the computing time and the memory space required for computation are considerably reduced. By this method the continuity equation is perturbed with a small term containing the pressure as given by the following equation:

$$\varepsilon p + \nabla \cdot \vec{u} = 0. \tag{22}$$

The perturbation parameter $\varepsilon$ must be chosen such that the product $\varepsilon p$ is of the order $10^{-6}$ [30,32]. The Navier–Stokes equations (7) and (8) are discretized with the standard Galerkin approach [33,34] and after the elimination of the pressure from the Navier–Stokes equations, the following set of non-linear algebraic equations are obtained:

$$\boldsymbol{M}\frac{\partial\vec{u}}{\partial t}+\boldsymbol{S}\vec{u}+\boldsymbol{N}(\vec{u})\vec{u}+\frac{1}{\varepsilon}\boldsymbol{L}^{\mathrm{T}}\boldsymbol{M}_p^{-1}\boldsymbol{L}\vec{u}=\boldsymbol{F}, \tag{23}$$

where $\vec{u}$ represent the discretized velocity vector, $\boldsymbol{S}$ the stress matrix which is a function of velocity for a generalized Newtonian fluid, $\boldsymbol{N}(\vec{u})$ the discretization of the convection terms, $\boldsymbol{L}$ the continuity matrix, $\boldsymbol{L}^{\mathrm{T}}$ the transpose of the continuity matrix, $\boldsymbol{M}$ the mass matrix, $\boldsymbol{M}_p$ the pressure matrix, $p$ the unknown pressure, $\tau = 1/\varepsilon$ the penalty parameter, and $\boldsymbol{F}$ the vector containing the boundary conditions. The pressure is obtained as a derivative of the velocity through the expression:

$$p = -\tau\boldsymbol{M}_p^{-1}\boldsymbol{L}\vec{u}. \tag{24}$$

The solution of the concentration field is obtained by using the velocity field obtained in Eq. (23). The time dependent term of the equation is solved using the Crank Nicolson method to improve the accuracy in time. The upwind technique was also employed in the solution of Eq. (23) to reduce the numerical oscillation due to the dominant effect of convection [32]. The simulated area is discretized into many isoparametric triangular elements with each element having six nodal points. Fig. 2 shows an example of the finite-element grid system used in computations. The linearization of Eq. (23) is done through Newton's iteration method. This method converges quadratically, but a good initial estimate is required, which is obtained by solving the Stokes equations and next by iterating the equations through Picard's iteration method [32].

## 4. Discussion of results

### 4.1. Validity of the results

The accuracy of numerical simulation depends very strongly on the number of nodal point used in the computation. Table 1 presents the results of the simulation for a stagnant drop for $Fo_{\mathrm{d}} = 0.1$. The analytical solution of the dimensionless mean concentration at this Fourier number as given by the model from Newton [8] and by Eq. (8) of the article from Henschke and Pfennig [3] is 0.229526. Comparing the simulated results with the analytical solution, it can be seen that as the number of nodal points increases, the accuracy of the simulation improves significantly. With a total nodal point of 2677, the agreement of the results with the analytical solution is very good. The actual computations were done with a total of 2304 isoparametric triangular elements which corresponds to a total of 4721 nodal points. The solution of convection–diffusion equation by large value of Reynolds numbers $Re_{\mathrm{c}}$ actually required fine grid which means that one need a small time step for numerical stability reasons [35]. The results of the simulations in this work, with the grid stated above, in the considered range of Reynolds number ($0 \leqslant Re_{\mathrm{c}} \leqslant 20$), are very good.

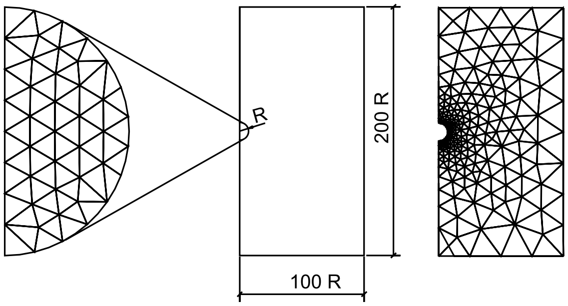

Fig. 2. An example of finite element grid system inside and outside the liquid drop.

Table 1
Effect of the number of nodal point on the accuracy of the simulated mass transfer by $Fo_{\mathrm{d}} = 0.1$ and $Re_{\mathrm{c}} = 0$

| Number of nodal point | Average concentration in drop | Percentage error |
|---|---|---|
| 317 | 0.234579 | 2.2015 |
| 1209 | 0.231364 | 0.8008 |
| 2677 | 0.230684 | 0.5045 |
| 4771 | 0.230552 | 0.4470 |

### 4.2. Mass expansion coefficient

In this work, the numerical investigations were carried out by using *n*-butyl-acetate–acetone–water, one of the standard test systems recommended by Misek et al. [36] for liquid–liquid extraction studies, as a case study. The required transport properties of the system are given in Table 2. The mass expansion coefficient used for the simulation of the mass transfer by free and combined convection was obtained through the relation:

Table 2
Transport properties for *n*-butyl-acetate and water by a temperature of 20 °C

| Substance | Viscosity $\eta$ $10^{-3}$ (kg/m s) | Density $\rho$ (kg/m$^3$) | Diffusion coefficient $D$ of acetone $10^{-9}$ (m$^2$/s) |
|---|---|---|---|
| Water | 1.003 | 998.2 | 1.093 |
| *n*-Butyl-acetate | 0.7300 | 881.5 | 2.200 |

$$\beta_{Ki} = -\frac{1}{\rho_i}\frac{\Delta\rho_i}{\Delta w_i}, \tag{25}$$

where $i$ represents the phase, $\rho_i$ the density of the pure system and $\Delta\rho_i$ the change in density due to changes in the mass fraction $\Delta w_i$. By correlating the density with the mass fraction up to 17%, the mass expansion coefficient for the dispersed phase was obtained as $\beta_{Kd} = 0.106$ and for the continuous phase as $\beta_{Kc} = 0.136$. The drop diameter was kept constant at 2 mm throughout the simulations. It should be noted that a *n*-butyl-acetate drop with a diameter of 2 mm sedimenting in water at a temperature of 20 °C, does so at a Reynolds number of 120. But the simulations in this work was carried out in the flow regime $0 < Re_c \leqslant 20$. This was to give room for the comparison of the effect of the combined free and forced convection with the effect of forced convection on the mass transfer, since the effect of combined free and forced convection on the mass transfer is only limited to this flow regime $Re_c \leqslant 20$ [37].

### 4.3. Average concentration

The average concentration in the drop at the beginning of the transport process is 10%. This reduces in value with time due to the mass transfer from the drop to the continuous phase.

Fig. 3 presents the changes in average concentration with time for mass transfer by diffusion, free, forced, and combined free and forced convection. Results show that free convection enhances mass transfer over the pure diffusion. Both for $Re_c = 5$ and 20, the mass transfer by forced convection is more than that by the combined free and forced convection for a rising drop. This is foremost surprising because the results is not in agreement with the previous results for the continuous phase mass transfer of a solid sphere. Pearson and Dickson [22] and Hanel [38] show that the combined free and forced convection of a falling solid sphere enhances mass transfer while the combined free and forced convection for a rising solid sphere suppresses mass transfer over the transfer by forced convection only.

To explain the new results, the velocity profiles at the equator plane both for forced, and combined free and forced convection for a falling drop for $Re_c = 5$ and $Fo_d = 0.0528$ (24 s) are compared with each other in Fig. 4. The curves show that the velocity at the centre of the drop ($r^* = 0$) for the combined free and forced convection is about two times that of the forced convection, but the velocity at the interface for both cases are about the same. The figure also indicates that the point of zero velocity (centre of the internal vortex) for the combined free and forced convection is $0.401R$ from the drop interface, while it is $0.293R$ in the case of forced convection. The diffusive distance to be overcome by mass transfer from the drop in the first case is thus higher than that for the second case. That leads to the poor mass transfer for the combined free and forced convection.

The effect of the direction of free convection on mass transfer was also examined. The mean concentration for $Re_c = 5$ by mass transfer through the combined free and forced convection for a falling and a rising drop was plotted over time in Fig. 5. For comparison purposes, the mean concentration for mass transfer by forced convection is also presented. The figure contains additionally the theoretical maximum possible mass transfer according to the model of Kronig and Brink [10]. The diagram shows that the mass transfer by the combined free and force convection for a rising drop impairs mass transfer. The amount of mass transfer by the above mentioned three cases is smaller than the theoretical model from Kronig and Brink.

In Fig. 6, the average Sherwood number was plotted over the Fourier number for the mass transfer by various flow conditions considered in this work. Curve a in the figure is valid for the Sherwood number for pure

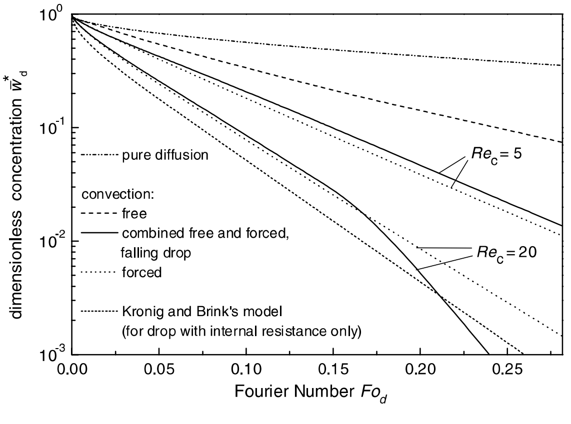

Fig. 3. Average concentration of a *n*-butyl-acetate drop as a function of time.

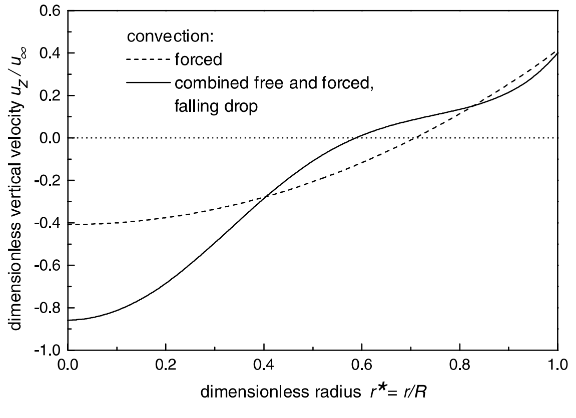

Fig. 4. Velocity profile along the equator plane inside a *n*-butyl-acetate drop for $Re_c = 5$ and $Fo_d = 0.0528$ (24 s).

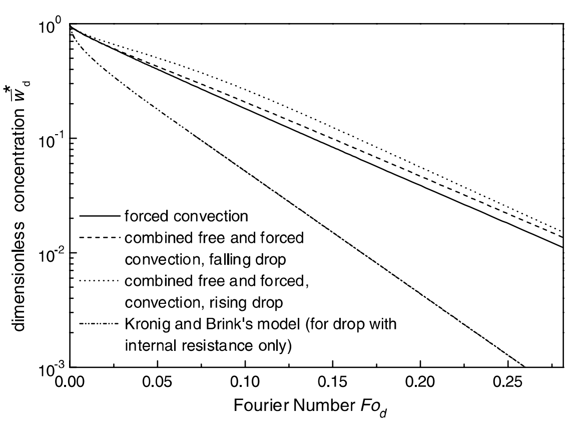

Fig. 5. Effect of the direction of free convection in a combined convection flow for $Re_c = 5$ in relation with time.

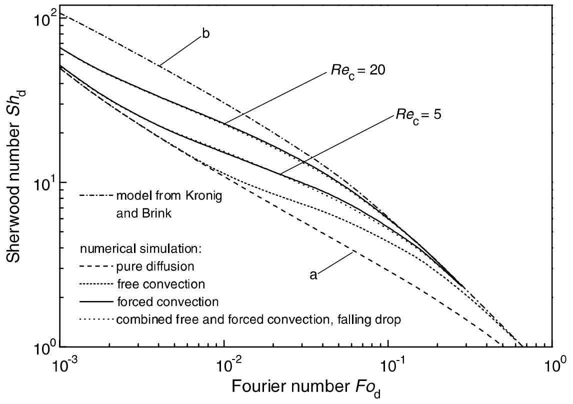

Fig. 6. Average Sherwood number of *n*-butyl-acetate drop in relation with the Fourier number.

diffusion. The curve depicts the lower limit and curve b, which corresponds to the model of Kronig and Brink, depicts the upper limit. Other curves for mass transfer by forced, and combined free and forced convection run from the curve a by small Fourier number over the curve b by high Fourier number. This trend, which is in agreement with the model of Kronig and Brink, shows that by corresponding high Fourier number, the circulation in the drop is complete. The curves further show that the superimposition of either free convection on forced convection does not have appreciable effect on the dispersed phase mass transfer. Furthermore, the curves which is in agreement with the results of Brauer [39] show that the average Sherwood number tends to zero when the Fourier number tends towards infinity.

## 5. Conclusions

The mass transfer process was described in this work by solving the complete Navier–Stokes and the convection–diffusion equations using the finite element method. The Navier–Stokes equations were modified through the Boussinesq-approximation to account for the effect of changes in density with concentration. The mass transfer was thus investigated for stagnant drop, free, forced and combined convection. The results show that the superimposition of free convection on forced convection does not enhances mass transfer but rather suppresses it. The small rate of mass transfer by the combined free and forced convection for a falling drop in comparison with the mass transfer by forced convection can be due to the effect of the continuous phase buoyancy force on the drop. With the help of the numerical simulation, the work has contributed to knowledge by answering an important technical question on the effect of combined convection on mass transfer.

## Acknowledgements

M.A. Waheed, one of the authors, thanks the German academic exchange service (DAAD) for the scholarship award for his doctoral research work at the Aachen University of Technology (RWTH), Aachen Germany.

## References

[1] A.S. Kumar, S. Hartland, Correlations for prediction of mass transfer coefficient in single drop systems and liquid–liquid extraction columns, Trans. IChemE Part A 77 (1999) 372–384.

[2] A.R. Uribe-Ramirez, W.J. Korchinsky, Fundamental theory for prediction of single-component mass transfer in liquid drops at intermediate Reynolds numbers $10 \leqslant Re \leqslant 250$, Chem. Eng. Sci. 55 (2000) 3305–3318.

[3] M. Henschke, A. Pfennig, Mass-transfer enhancement in single-drop extraction experiments, AIChE J. 45 (10) (1999) 2079–2086.

[4] C.V. Sternling, L.E. Scriven, Interfacial turbulence: hydrodynamic instability and the Marangoni effect, AIChE J. 5 (4) (1959) 514–519.

[5] S. Wolf, J. Stichlmair, The Marangoni-effect during mass transfer in liquid–liquid systems, In: Preprints of the 12th International Congress of Chemical and Process Engineering (Chisa), Praha, Czech Republic, 25–30 August, 1996.

[6] R. Clift, J.R. Grace, M.E. Weber, Bubbles, Drops and Particles, Academic Press, New York, 1978.

[7] H. Gröber, Die Erwärmung und Abkühlung einfacher geometrischer Körper, Z. Ver. Dtsch. Ing. 69 (21) (1925) 705–711.

[8] A.B. Newman, The drying of porous solids: diffusion calculation, Trans. AIChE 27 (1931) 310–332.

[9] F. Cooper, Heat transfer from a sphere to an infinite medium, Int. J. Heat Mass Transfer 26 (1977) 991–993.

[10] R. Kronig, J.C. Brink, On the theory of extraction from falling droplets, Appl. Sci. Res. A 2 (1950) 142–154.

[11] B.I. Brounshtein, A.S. Zheleznyak, G.A. Fishbein, Heat and mass transfer in interaction of spherical drops and gas

bubbles with a liquid flow, Int. J. Heat Mass Transfer 13 (1970) 963–973.

[12] E. Ruckenstein, Mass transfer between a single drop and a continuous phase, Int. J. Heat Mass Transfer 10 (1967) 1785–1792.

[13] B.T. Chao, Transient heat and mass transfer to a translating droplet, J. Heat Transfer C 91 (2) (1969) 273–281.

[14] U.J. Plöcker, H. Schmidt-Traub, Instationärer stofftransport zwischen einer einzelkugel und einer ruhenden umgebung, Chem. Ing. Tech. 44 (5) (1972) 313–319.

[15] G.H. Juncu, R. Mihail, The effect of diffusivities ratio on conjugate mass transfer from a droplet, Int. J. Heat Mass Transfer 30 (6) (1987) 1223–1226.

[16] J.S. Hadamard, Mouvement permanent lent d'une sphère liquide et visqueuse dans un liquide visqueux, Compt. Rend. Acad. Sci. 152 (1911) 1735–1743.

[17] W. Rybczynski, Über die fortschreitende Bewegung einer flüssigen Kugel in einem zähen medium, Bull. Int. Acad. Sci. Cracovie, Ser. A (1911) 40–46.

[18] E.R. Elzinga Jr., J.T. Banchero, Film coefficients for heat transfer to liquid drops, Chem. Eng. Prog. Symp. Ser. 29 (55) (1959) 149–161.

[19] A. Acrivos, Combined laminar free and forced convection heat transfer in external flows, AIChE J. 4 (3) (1958) 285–289.

[20] F.H. Garner, J.M. Hoffman, Mass transfer from single solid spheres by free convection, AIChE J. 7 (1) (1961) 148–152.

[21] R.L. Steinberger, R.E. Treybal, Mass transfer from a solid soluble sphere to a flowing liquid stream, AIChE J. 6 (2) (1960) 227–232.

[22] R.S. Pearson, P.F. Dickson, Free convective effects on stokes flow mass transfer, AIChE J. 14 (14) (1968) 903–908.

[23] L.D. Landau, E.M. Lifschitz, Lehrbuch der thereoretischen Physik, Band VI: Hydrodynamik, Akademik Verlag, Berlin, 1991.

[24] H. Schlichting, K. Gersten, Grenzschicht—Theorie, 9 Aufl, Verlag G. Braun, Karlsruhe, 1997.

[25] A. Oberbeck, Über die Wärmeleitung der Flüssigkeiten bei Berücksichtigung der Strömungen infolge von Temperaturdifferenzen, Ann. Phys. Chem. 7 (1879) 271–292.

[26] M.J. Boussinesq, Théorie Analytique de la Chaleur, vol. 2, Gauthier-Vilaris, Paris, 1903.

[27] R.B. Bird, W.E. Stewart, E.N. Lightfoot, Transport Phenomena, John Wiley, New York, London, 1960.

[28] L. Hilprecht, Instationärer impuls- und stoffaustauch bei beschleunigter bewegung von einzelpartikeln, VDI—Forschungsheft: VDI—Verlag, Düsseldorf, 1976.

[29] H. Brauer, Unsteady state mass transfer through the interface of spherical particles-I, Int. J. Heat Mass Transfer 21 (1978) 445–453.

[30] SEPRAN A Finite Element Code, Ingenieursbureau Sepra, Leidschendam, Niederlande, 1999.

[31] K.J. Bathe, Finite-Elemente-Methoden, Spinger Verlag, Berlin, 1986.

[32] C. Cuvelier, A. Segal, A.A. van Steenhoven, Finite Element Methods and Navier–Stokes Equations, D. Reidel Publishing Company, Dordrecht, Holland, 1986.

[33] T.J. Chung, Finite Elemente in der Strömungsmechanik, Hanser Verlag, München, Wien, 1983.

[34] T.E. Tezduyar, D.K. Ganjoo, Petrov–Galerkin formulations with weighting functions dependent upon spatial and temporal discretization: application to transient convection diffusion problem, Comput. Meth. Appl. Mech. Eng. 59 (1986) 49–71.

[35] S.S. Ponoth, J.B. McLaughlin, Numerical simulation of mass transfer for bubbles in water, Chem. Eng. Sci. 55 (2000) 1237–1255.

[36] T. Misek, R. Berger, J. Schröter (Eds.), European Federation of Chemical Engineering. Standard Test Systems for Liquid Extraction, second ed., The Institution of Chemical Engineers, Warwickshire, 1985.

[37] H. Schmidt-Traub, Impuls- und Stoffaustausch an umströmten Kugeln unter Berücksichtigung der inneren Zirkulation und der freien Konvektion, Ph.D. thesis, Technical University, Berlin, 1970.

[38] B. Hanel, Einführung in die konvektive Wärme- und Stoffübertragungfirst, first ed., Verlag Technik, GmbH Berlin, 1990.

[39] H. Brauer, Stoffaustausch einschließlich chemischer Reaktionen, Verlag Sauerländer, Aarau und Frankfurt am Main, 1971.